# Transmission properties of all-silica fibres for high-power Nd:YAG lasers

N. RENG, T. BECK

The transmission properties of two different types of all-silica fibres, step index and graded-index fibres, are investigated using a multimode high-power cw Nd:YAG rod laser. The reflections from the fibre surface back into the laser cavity affect the laser power and the beam parameters, waist diameter and divergence. A set-up for simultaneously measuring these values in front of and behind a fibre is presented. The maximum laser power transmitted by fibres is dependent upon the beam parameters, the fibre design and the surface conditions. An upper limit for the maximum divergence which can be coupled into a fibre with a certain numerical aperture without loss is given. The beam parameters behind the fibre, related to the input parameters, are presented.

KEYWORDS: lasers (Nd:YAG), all-silica fibres

## Introduction

Fibres for high power Nd:YAG laser transmission are in industrial use in the field of materials processing.[1-4] Meanwhile more than 2 kW laser power can be transmitted through all-silica fibres (Table 1). For industrial applications it is of major interest to know the beam parameters, waist diameter $d$ and divergence $\theta$ (full angle), behind the fibre in order to be able to focus the beam to a certain spot size with a certain focal depth. For this reason it is necessary to investigate the dependency of the fibre output beam parameters upon the input parameters and the fibre geometry. The fibres compared in the experiments are described in Table 2. They consist of

The authors are at the Festkørper-Laser-Institut Berlin GMBH, Straße des 17. Jun: 135, Postfach 12 64 11, 1000 Berlin 12.
Received 1 October 1992. Revised 19 January 1993. Accepted 22 January 1992.

**Table 1. Transmission properties of step index (SI) and graded-index fibers (GI) with different lengths, core diameters $D_{core}$ and numerical apertures $NA$. (1) Data not available; (2) data read from transmission curves; (cw) continuously operating laser system; (pw) pulsed laser system**

| Fibre | Length (m) | $D_{core}$ ($\mu$m) | $NA$ | Fibre input power $P_{laser}$ (W) | Fibre output power $P_{fibre}$ (W) | $P_{fibre}/P_{laser}$ | |
|---|---|---|---|---|---|---|---|
| SI | 200 | 680 | 0.20 | ≈1750 cw (2) | ≈1550 cw (2) | ≈0.89 | Ref 1 |
| | | | | ≈1770 pw (2) | ≈1500 pw (2) | ≈0.85 | |
| GI | 200 | 550 | 0.25 | ≈1200 cw (2) | ≈1050 cw (2) | ≈0.88 | |
| | | | | ≈1650 pw (2) | ≈1500 pw (2) | ≈0.91 | |
| | 5 | 400 | | ≈1000 pw (2) | ≈940 pw (2) | ≈0.94 | |
| SI | (1) | 1000 | 0.17 | 2150 cw | 1900 | 0.88 | Ref 2 |
| | (1) | 600 | | 1820 cw | 1600 | 0.88 | |
| | (1) | 400 | | 1150 cw | 1050 | 0.91 | |

0030-3992/93/020117-08 © 1993 Butterworth-Heinemann Ltd

**Table 2. Data of the fibres compared in the experiments; $n_{buff}$: refractive index of the plastic buffer, $n_{core}$: refractive index of the fiber core, $n_{clad}$: refractive index of the fibre cladding**

| | Step index fibre | | Graded-index fibre | |
|---|---|---|---|---|
| Core diameter, $D_{core}$ ($\mu$m) | 400 | 600 | 400 | 600 |
| Cladding diameter, $D_{clad}$ ($\mu$m) | 480 | 660 | 550 | 850 |
| Numerical aperture, *NA* | 0.22 | | 0.25 | |
| Length (m) | $\approx$2.5 | $\approx$20 | $\approx$5 | $\approx$20 |
| Buffer material | acrylate | silicone | silicone | |
| Refractive indices | $n_{clad} < n_{core} < n_{buff}$ | $n_{buff} < n_{clad} < n_{core}$ | $n_{buff} < n_{clad} < n_{core}$ | |

differently doped silica core and cladding, thus forming a characteristic refractive index profile, covered with a plastic buffer to increase the mechanical strength and the chemical resistance of the silica material.[5] According to their core refractive index profile, they are called step index or graded-index fibres. Other step index fibre samples with 660 to 840 $\mu$m cladding diameter are used to investigate the influence of spherical coupling surfaces.

For measuring the fibre transmission properties a cw Nd:YAG rod laser system is used with a maximum output power of approximately 300 W. It consists of an 8 mm diameter and 152.4 mm long rod in a 50 cm long, symmetrical resonator with plane mirrors. The rod lies in the focal line of an elliptical, gold-layered cavity, which is pumped by one krypton arc lamp in the other focal line with 10 kW at maximum electric power. Because of the pumping geometry the contours of the laser beam are more or less elliptical. The lasers in the set-ups are built with up to six cavities in a line with equal distances between the cavities, thus conserving the beam parameter product, but scaling up the output power.[6,7] The output power of the six-cavity laser with six 45 cm long resonator modules reaches 1.9 kW cw.

All beam parameters are determined with the set-up described in the next section. At low pumping powers behind the fibre, more laser power is observed than without the fibre, which is due to the reduction of the laser threshold by fibre feedback. A simple theoretical model and measurements are described in the third section. In order to be able to compare reliably the fibre input and output power and beam parameters, these quantities are measured simultaneously. The experimental set-up and results

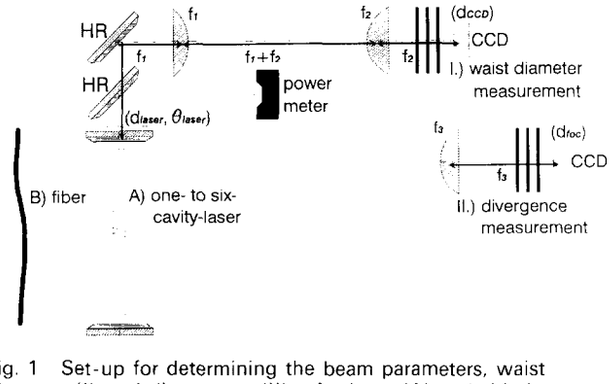


Fig. 1 Set-up for determining the beam parameters, waist diameter (I) and divergence (II), of a laser (A) or behind a fibre (B) with a telescopic system

are presented in the fourth section. Finally, some remarks and observations concerning the fibre end face preparation are made.

## Measurement of the beam parameters

The beam parameters, waist diameter $d$ and divergence $\theta$, are measured in the set-up shown in Fig. 1. It allows one to compare the beam parameters of the laser radiation field at the fibre input and the fibre output simultaneously. The beam waist diameter $d_{laser}$ at the output mirror is determined with a CCD-camera behind a telescopic system, which reproduces the size of the beam in the ratio of the focal lengths $f_1$ and $f_2$ of the telescopic lenses:

$$d_{laser} = \frac{f_1}{f_2} d_{CCD} \tag{1}$$

The divergence $\theta_{laser}$ is calculated from the beam diameter $d_{foc}$ at focal length distance $f_3$ from the third lens placed behind the telescopic system.

$$\theta_{laser} = \frac{f_2}{f_1} \frac{d_{foc}}{f_3} \tag{2}$$

The telescopic system is correctly adjusted, if the waist $d_{CCD}$ remains at the position of the CCD-camera regardless of the pumping power. The diameter $d_{foc}$ behind the third lens must be independent from the distance of the third lens to the telescopic system. With not exactly aligned lenses or a CCD-camera, the error can become very large.

The product of half the waist diameter $d/2$ and half the divergence $\theta/2$ is the beam parameter product. It is constant in perfect optical systems. Two definitions of the beam diameter are applied.[8,9] The first is defined by the circle whose diameter $d$ includes 98% of the beam power. It ensures that the fibre is not destroyed when a high power laser beam, with diameter $d_{in}$ and divergence $\theta_{in}$, is coupled into a fibre close to its acceptance limits, core diameter $D_{core}$ and numerical aperture $NA$. The second definition is applied to more or less elliptical beams with different beam diameters at two orthogonal directions. It is given by the 95.4% power contents within a slit of length $d_x$ and $d_y$, added up along the principal axes of the intensity distribution of the laser beam in the horizontal and vertical direction. For a Gaussian beam this definition yields the Gaussian beam diameter with 86.5% of the total beam power encircled. This definition is only applied in the next section when the influence of the reflections from the fibre end faces is investigated.

Other telescopic systems are used for determining the beam parameters behind fibres, for coupling the laser beam into fibres or for investigating the fibre end face reflections. The beam diameters and divergences are scaled by the ratio $f_1/f_2$.

## Fibre end face reflections

The laser threshold, the laser output power and the beam parameters are influenced by back reflections from the fibre end faces. For fibre transmission and material processing the effects due to back reflections mean an uncertainty for the coupling and the processing parameters. The laser output mirror and the additional, reflecting plane are regarded as an external Fabry-Perot cavity, which is coupled with the laser cavity.[10–12] In resonance, the coupled cavities can be described as one laser cavity with an effective reflection coefficient $R_{\text{eff}}$ of the output mirror

$$R_{\text{eff}} = \left( \frac{\sqrt{R_1} + \sqrt{R_2}}{1 + \sqrt{R_1 R_2}} \right)^2 \tag{3}$$

where $R_1$ is the reflection coefficient of the laser output mirror, and $R_2$ is the reflection coefficient of the additional surface. For investigating the influence of the back reflections of one fibre end face, it is compared with a prism surface. In the experimental set-up the reflection coefficient $R_1$ is 75%, $R_{2,\text{prism}}$ of the prism surface is 4.1% and $R_{2,\text{fibre}}$ of both fibre end faces is approximately 6.5%, this leads to an effective reflection coefficient $R_{\text{eff,prism}}$ for the laser mirror–prism set-up of about 83%, which is comparable with the $R_{\text{eff, fibre}}$ of the laser mirror–fibre set-up of about 84%.

With a telescopic system the laser beam is focused onto a prism and a step index fibre. Simultaneously, the laser beam parameters are measured[9] (Fig. 2). Figure 3 shows the normalized laser output power $P_{\text{laser}}/P_{\text{laser,max}}$ against the reflection coefficient $R_1$ of the laser output mirror at two pumping power levels.[10] The dashed curves denote the reflection coefficient $R_1$ and the effective reflection coefficient $R_{\text{eff,prism}}$ according to (3) and the corresponding laser output power. The normalized laser output power $P_{\text{laser}}/P_{\text{laser,max}}$ when moving the prism out of the beam waist is presented in Fig. 4. Then, the beam portion reflected at the prism surface does not coincide with

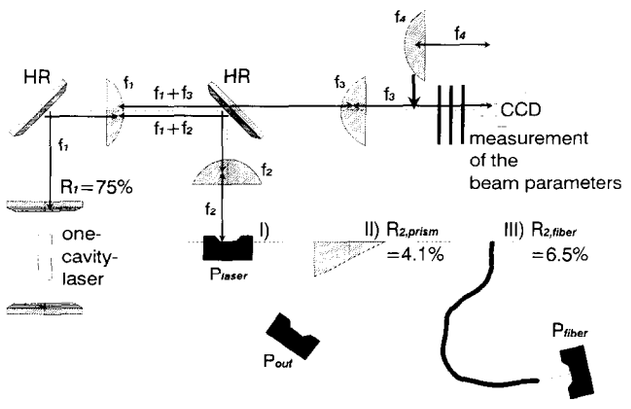


Fig. 2 Set-up for investigating the influence of prism (II) and fibre end face reflections (III) and simultaneously recording the beam parameters

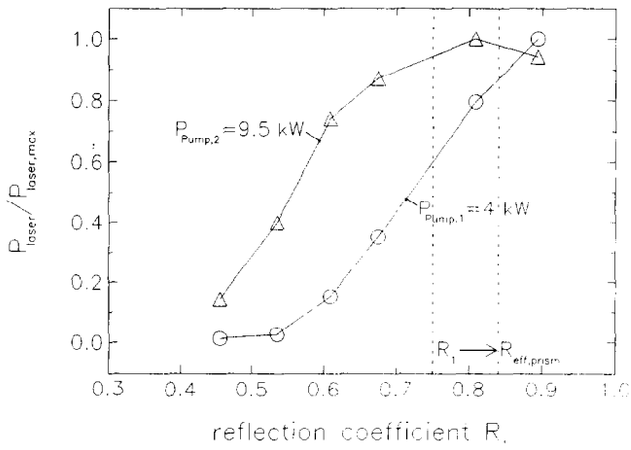


Fig. 3 Normalized laser output power $P_{\text{laser}}/P_{\text{laser,max}}$ dependent upon the reflection coefficient $R_1$ of the laser output mirror. The dashed lines denote the prism reflections which lead to an effective reflection coefficient $R_{\text{eff,prism}}$ and affect the laser output power

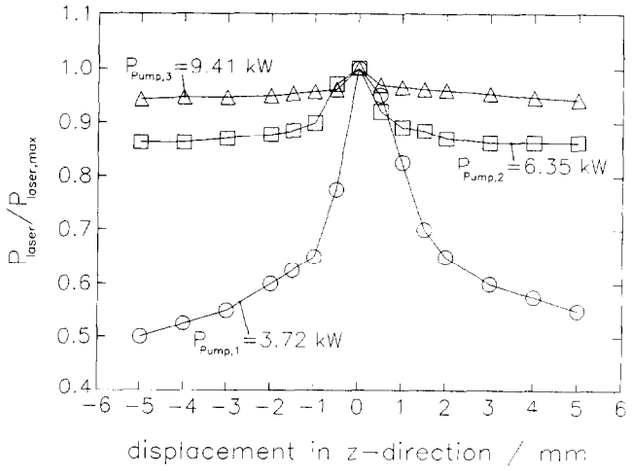


Fig. 4 Normalized laser output power $P_{\text{laser}}/P_{\text{laser,max}}$ dependent upon the prism position, the prism moved out of the beam waist at $z = 0$ for three pumping powers, $P_{\text{pump,1}} = 3.72$ kW, $P_{\text{pump,2}} = 6.35$ kW and $P_{\text{pump,3}} = 9.41$ kW. Maximum laser power is achieved, when the prism is placed at the beam waist.

the laser output beam, the laser cavity and the external laser mirror–prism cavity are more and more off-resonance and, especially at low pumping powers $P_{\text{pump}}$, the laser output power $P_{\text{laser}}$ decreases. Figure 5

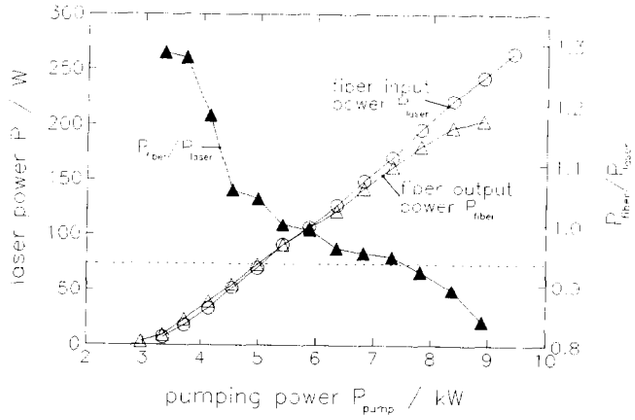


Fig. 5 'Transmission' $P_{\text{fibre}}/P_{\text{laser}}$ of the 400 $\mu$m step index fibre not regarding the influence of the fibre end face reflections. The influence is biggest at low pumping powers $P_{\text{pump}}$

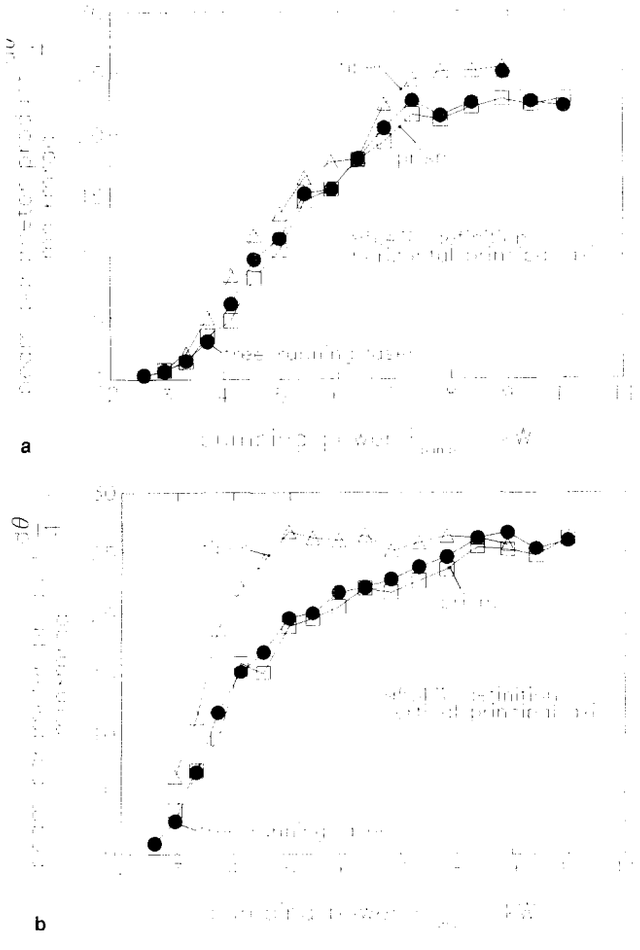

Fig. 6 Influence of the beam parameter product $d\theta/4$ in the (a) horizontal and (b) vertical principal axis of the laser beam with prism and fibre end face reflections, both elements placed in the beam waist

shows the 'transmission' $P_{\text{fibre}}/P_{\text{laser}}$ of the 400 $\mu$m step index fibre (Table 2) with the fibre being adjusted to obtain maximum output power $P_{\text{laser}}$ (cf. Fig. 4). The dashed curve denotes the theoretical, upper limit $P_{\text{fibre}}/P_{\text{laser}}$ of 0.935. Because the laser power, and so the fibre transmission, are affected, for correct

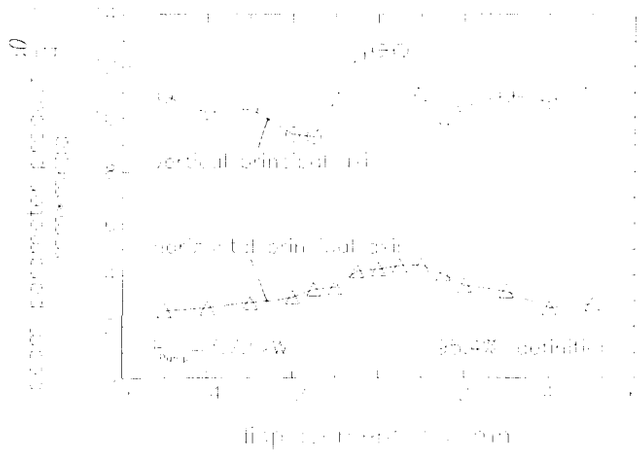

Fig. 7 Beam parameter product $d\theta/4$ in the horizontal and vertical principal axis of the laser beam with prism reflections, the prism moved out of the beam waist at $z = 0$

determination the fibre input and output powers must be measured simultaneously.

Figures 6(a) and (b) show the beam parameter product $d\theta/4$ in the horizontal and vertical principal axes at prism and fibre end face reflections, with the prism and the fibre being adjusted for maximum laser power $P_{\text{laser}}$ in order to be sure to place the prism and the fibre at the beam waist (cf. Fig. 4). At the prism surface the laser beam is reflected on itself, if the beam waist is located at the prism surface. Therefore, although the laser output power is strongly influenced as described above, the beam parameters remain nearly unaffected. However, when moving the prism only some millimetres out of the beam waist, the beam parameters are influenced, because the beam is not reflected on itself (Fig. 7, cf. Fig. 4). When coupling the laser beam into the step index fibre the beam is reflected at both fibre end faces, which affects the beam parameter product $d\theta/4$, because, after transmission through a step index fibre, the beam parameters increase. Therefore, the beam reflected at the fibre end faces does not coincide with the beam of the free-running laser without the fibre. In the horizontal direction the beam qualities of the free-running laser and of the laser with the beam focused onto the fibre end face seem to coincide. However, the beam parameters, diameter $d$ and divergence $\theta$, are different, but the product $d\theta/4$ is, by chance, equal. So, for comparing the beam parameters in front of and behind a fibre the corresponding figures must be measured simultaneously, too. The experimental set-ups will be presented in the next section.

## Fibre transmission properties

Treating the multimodal laser radiation field with diameter $d$ and divergence $\theta$ as infinitely thin rays with corresponding distance $d$ from the beam axis and angle $\theta$ launched into the core of a step index fibre, the geometrical picture leads to the coupling conditions for lossless laser beam transmission within the fibre.[13-15] The beam diameter $d_{\text{in}}$ and divergence $\theta_{\text{in}}$ (full angle) at the fibre-coupling surface are thus constrained by the fibre core diameter $D_{\text{core}}$ and numerical aperture $NA$:

$$\left.\begin{aligned} d_{\text{in}} &\leqslant D_{\text{core}} \\ \theta_{\text{in}} &\leqslant 2\arcsin(NA) \end{aligned}\right\} \tag{4}$$

The rays are totally reflected at the core-cladding interface, resulting in a zigzag path. Because of the different optical path lengths for every ray at the end of the fibre the core is entirely filled by the laser beam, the beam diameter $d_{\text{out}}$, being independent of the beam diameter $d_{\text{in}}$ coupled into the fibre. Due to the internal total reflections the output divergence $\theta_{\text{out}}$ remains approximately constant:

$$\left.\begin{aligned} d_{\text{out}} &\approx D_{\text{core}} \\ \theta_{\text{out}} &\approx \theta_{\text{in}} \end{aligned}\right\} \tag{5}$$

A ray in the core of a graded-index fibre with a parabolic refractive index profile is smoothly bent,

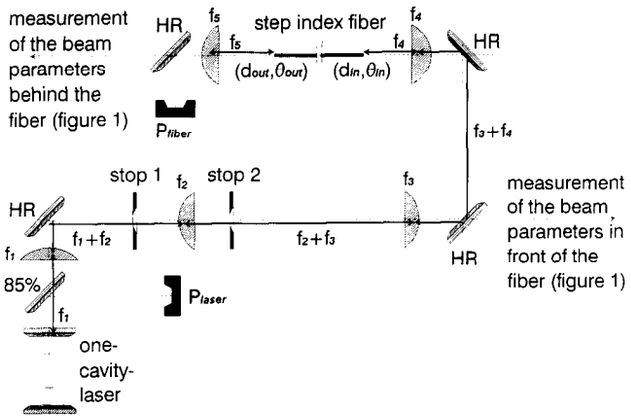


Fig. 8 Set-up for investigating the coupling conditions (4). The beam powers and the beam parameters in front of and behind the fibre are measured simultaneously

when approaching the core-cladding interface, therefore showing an undulating ray propagation. According to Refs 13, 14, 16 and 17 the index profile, resulting in equal optical path lengths for every ray, depends upon the launching conditions. There exist different, slightly deviating solutions for rays, which pass the fibre axis after every bend (meridional rays: hyperbolic secant refractive index profile), and other rays, which never cross the fibre axis (skew rays: Lorentzian refractive index profile). Furthermore, because of the finite core size the results of these calculations are more or less idealized. So, when placing the fibre at the beam waist, the following equations are only rough approximations:

$$\left.\begin{aligned} d_{out} &\approx d_{in} \\ \theta_{out} &\approx \theta_{in} \end{aligned}\right\} \qquad (6)$$

This relation holds, if the distortions due to inhomogeneities and bending of the fibre are negligible.

## Testing the coupling conditions

Maximum transmission should be obtained, if the coupling conditions according to (4) are fulfilled. For

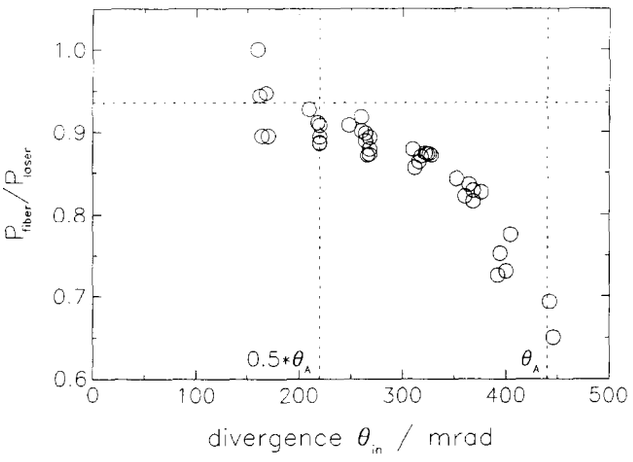


Fig. 9 Transmission $P_{fibre}/P_{laser}$ of the 400 $\mu$m step index fibre dependent upon the beam divergences $\theta_{in}$, most of them lying below the theoretical acceptance angle 2arcsin(NA). The decrease of the transmission is independent of the laser power $P_{laser}$

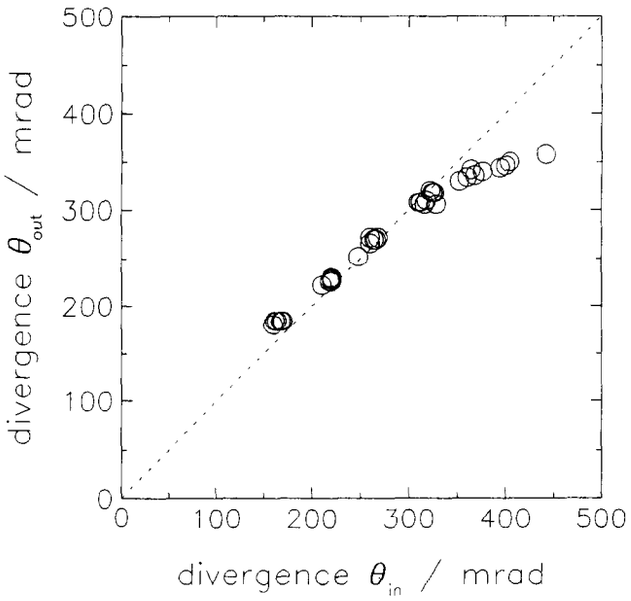


Fig. 10 Beam divergences $\theta_{out}$ behind the 400 $\mu$m step index fibre in comparison with the divergences $\theta_{in}$ coupled into the fibre. The decrease of the divergences $\theta_{out}$ is independent of the laser power $P_{laser}$

a step index fibre this is investigated with an attenuated laser beam in order to prevent the fibre from destruction, when the coupling conditions do not hold. The experimental set-up[9] is shown in Fig. 8. The beam diameter is adapted to the fibre core diameter with two telescopic systems. The divergence $\theta_{in}$ coupled into the fibre depends upon the pumping power but is limited by the first stop with various diameters $D_{stop}$ in the focal length distance $f_2$ in front of the second lens. So the maximum divergence $\theta_{in,max}$ can be obtained from the formula

$$\theta_{in,max} = \frac{f_3}{f_4}\,\frac{D_{stop}}{f_2} \qquad (7)$$

where $f_2$, $f_3$ and $f_4$ are the focal lengths of the lenses (cf. (2)). The second stop in the beam waist between the two telescopic systems blocks all beam portions with diameter $d_{in}$ larger than $D_{core}$. The related beam parameters and the beam powers in front of and behind the fibre are measured simultaneously.

It appears that beam portions with diameter $d_{in}$ less than the core diameter $D_{core}$ are transmitted without loss, but portions with beam divergences $\theta_{in}$ more than approximately arcsin($NA$); that is, half the acceptance angle, suffer increasing transmission losses (Fig. 9). It is independent of the laser power coupled into the fibre. The coupling conditions (4) must therefore be replaced by

$$\left.\begin{aligned} d_{in} &\leqslant D_{core} \\ \theta_{in} &\leqslant \arcsin(NA) \end{aligned}\right\} \qquad (8)$$

Part of the laser power is radiated off at, or shortly behind, the fibre-coupling surface (because of surface imperfections and because the laser radiation field does not exactly match all fibre propagation modes—see Refs 13 and 18) and along the fibre, because

**Table 3. Transmission properties of the step index and graded-index fibres of Table 2**

| Fibre | Step index fibre | | Graded-index fibre | |
|---|---|---|---|---|
| $D_{core}$ [$\mu$m] | 400 | 600 | 400 | 600 |
| $P_{laser,max}$ [W] | 549 | 795 | 993 | 1880 |
| $P_{fibre,max}$ [W] | 482 | 677 | 926 | 1780 |
| $P_{laser,max}/P_{fibre,max}$ | 0.88 | 0.85 | 0.93 | 0.95 |
| $d_{in,max}$ [$\mu$m] | 403 | 566 | 410 | 608 |
| $\theta_{in,max}$ [mrad] | 277 | 256 | 438 | 301 |
| $d_{out,max}$ [$\mu$m] | 408 | 658 | 530 | 668 |
| $\theta_{out,max}$ [mrad] | 264 | 310 | 478 | 410 |

propagation modes scatter into radiation modes at fibre imperfections.[18–20] In particular, beams with larger divergences than arcsin($NA$) consist of beam portions which are radiated off because of these reasons (Fig. 10). With high power lasers the buffer can catch fire and the fibre will be destroyed.

## Comparison of different fibres

The fibres investigated are those of Table 2. The first set-up for measuring the beam parameters and laser powers simultaneously in front of and behind the fibre is similar to that of Fig. 8 with a one or six-cavity laser. Only one telescopic system with lenses $f_1$ and $f_2$ and without stops is used; the beam-splitter $R = 85\%$ is omitted. The laser power $P_{laser}$ coupled into the fibre is determined with a pin-diode behind a high reflecting mirror in front of the fibre. It is calibrated to the power meter measuring the laser power $P_{fibre}$ behind the fibre for obtaining reproducible transmission values. The second set-up is a modified commercial lens configuration for high-power Nd:YAG lasers. It is used because of its higher mechanical stability and because originally it is designed as a coupling unit for the industrial use of the 600 $\mu$m graded-index fibre. The distances between the lenses are chosen in order to adjust any beam diameter $d_{in}$ at the fibre end face. The beam diameter $d_{laser}$ and divergence $\theta_{laser}$ at the laser output mirror are considered $N$ times the diffraction limited beam parameters $d_0$ and $\theta_0$, for which the ABCD-law holds.[21] The beam parameters $d_0$ and $\theta_0$ are transformed by the lens configuration according to

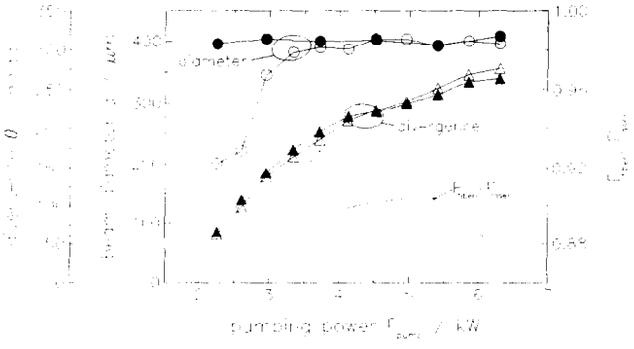

Fig. 11 Transmission properties of the 400 $\mu$m step index fibre with acrylate buffer; solid line: transmission $P_{fibre}/P_{laser}$; open circles: beam diameter $d_{in}$; closed circles: beam diameter $d_{out}$; open triangles: beam divergence $\theta_{in}$; closed triangles: beam divergence $\theta_{out}$; $P_{pump}$: pumping power per cavity

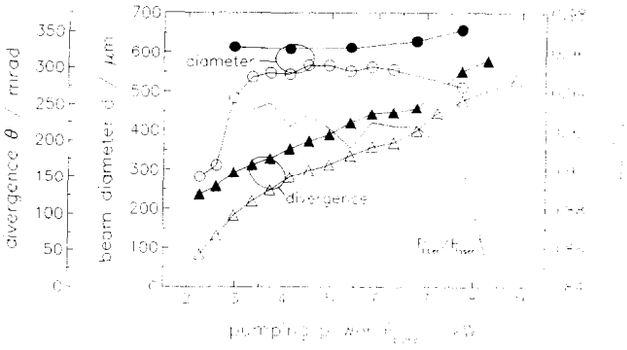

Fig. 12 Transmission properties of the 600 $\mu$m step index fibre with silicone buffer; solid line: transmission $P_{fibre}/P_{laser}$; open circles: beam diameter $d_{in}$; closed circles: beam diameter $d_{out}$; open triangles: beam divergence $\theta_{in}$; closed triangles: beam divergence $\theta_{out}$; $P_{pump}$: pumping power per cavity

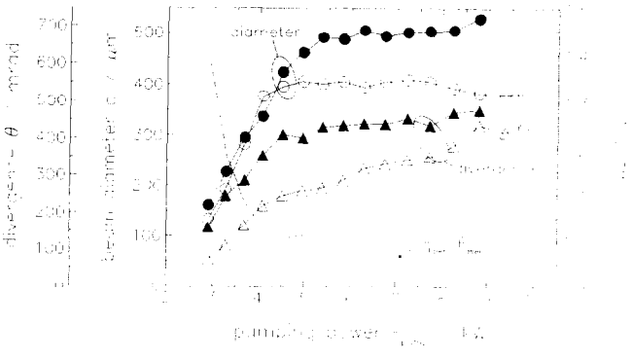

Fig. 13 Transmission properties of the 400 $\mu$m gradient index fibre with silicon buffer; solid line: transmission $P_{fiber}/P_{laser}$; open circles: beam diameter $d_{in}$; closed circles: beam diameter $d_{out}$; open triangles: beam divergence $\theta_{in}$; closed triangles: beam divergence $\theta_{out}$; $P_{pump}$: pumping power per cavity

the ABCD-formalism, and then multiplied with the factor $N$ to obtain the multimode beam parameters $d_{in}$ and $\theta_{in}$ at the fibre end face. The laser beam power and beam parameters are not measured simultaneously in front of and behind the fibre as described above. Therefore, the transmission figures $P_{fibre}/P_{laser}$ are subject to certain errors and the beam parameters cannot be compared directly.

The step index fibres are investigated with the first set-up, the 600 $\mu$m graded-index fibre with the second

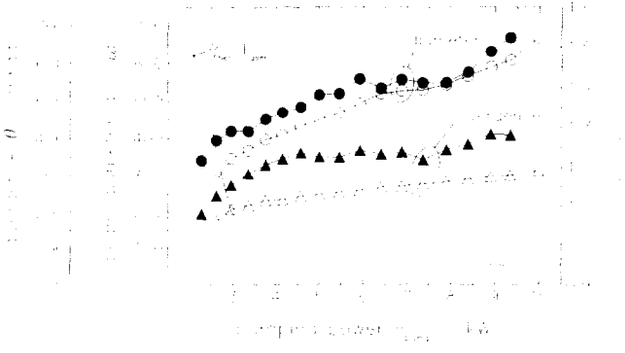

Fig. 14 Transmission properties of the 600 $\mu$m gradient index fibre with silicon buffer; solid line: transmission $P_{fibre}/P_{laser}$; open circles: beam diameter $d_{in}$; closed circles: beam diameter $d_{out}$; open triangles: beam divergence $\theta_{in}$; closed triangles: beam divergence $\theta_{out}$; $P_{pump}$: pumping power per cavity

one. However, the transmission figure $P_{fibre}/P_{laser}$ of the 400 $\mu$m graded-index fibre is measured with the second set-up by determining the laser power first in front of, and then behind, the fibre; that is, without taking the reflections from the fibre end faces into account, whereas the beam parameters are compared with the first set-up considering the fibre feedback. The results are summarized in Table 3 and Figs 11 to 14 (see Ref. 9).

The highest transmission figures $P_{fibre}/P_{laser}$ and laser powers $P_{laser}$ to be coupled into the fibre can be achieved when the maximum beam diameters $d_{in}$ approximately equal the core size $D_{core}$; consequently the beam divergence $\theta_{in}$ coupled into the fibre is minimized. This is done by choosing appropriate telescopic lenses in the first set-up or varying the distances between the lenses in the second one.

For the 400 $\mu$m step index fibre with an acrylate buffer (Fig. 11) equations (8) and (5) concerning the fibre input and output beam parameters are valid. The relations presented in Figs 9 and 10 also hold for high power lasers. The maximum beam power $P_{laser}$ to be transmitted is limited by the divergence coupled into the fibre. The fibre suffers increasing transmission losses when the fibre output divergence exceeds the input divergence.

All fibres with silicone buffer (Figs 12 to 14) have higher transmission values $P_{fibre}/P_{laser}$ than the acrylate-coated one, which can be read from the higher laser powers transmitted by these fibres (see Table 3) and the later decrease of transmission $P_{fibre}/P_{laser}$ at high pumping powers $P_{pump}$. However, the relations (5) and (6) between the input and output beam parameters only roughly hold. At high pumping powers $P_{pump}$ the output beam diameter $d_{out}$ exceeds the core diameter $D_{core}$. The divergence $\theta_{out}$ is larger than the divergence $\theta_{in}$ coupled into the fibre at all pumping powers and at high pumping powers also larger than $\arcsin(NA)$.

At high pumping powers the transmission $P_{fibre}/P_{laser}$ of the 600 $\mu$m step index fibre with silicone buffer (Fig. 12) falls. Because the refractive index $n_{buff}$ of the silicone buffer is lower than $n_{clad}$, the refractive index of the silica cladding, the cladding-coating layer is capable of acting as a wave-guiding structure. Therefore, at high pumping powers $P_{pump}$, at which the divergence $\theta_{in}$ exceeds the limiting angle $\arcsin(NA)$ according to (8), the beam diameter $d_{out}$ and the divergence $\theta_{out}$ at the end of the fibre are larger than the core diameter $D_{core}$ and the divergence $\theta_{in}$. However, due to the obviously low purity of the buffer material the transmission $P_{fibre}/P_{laser}$ at high pumping powers $P_{pump}$ rapidly decreases. Therefore, this fibre has no advantage over the acrylate-coated 400 $\mu$m step index fibre. The higher laser power transmitted can mainly be traced back to the larger core diameter $D_{core}$. Moreover the silicone-coated 600 $\mu$m step index fibre has the great disadvantage that the output beam diameter $d_{out}$ exceeds the core diameter $D_{core}$ at high pumping powers, which causes problems when the aim is to achieve a small spot with fixed diameter on the material over a wide range of laser power $P_{fibre}$.

The graded-index fibres exhibit the highest transmission values $P_{fibre}/P_{laser}$ and are capable of transmitting the highest laser powers $P_{laser}$. However, as expected, the preservation of the beam parameter product $d_{in}\theta_{in}/4$ according to (6) only approximately works. In particular, with the 400 $\mu$m graded-index fibre (Fig. 13), the wave-guiding function of the silica cladding and the silicone buffer can be observed, because the beam parameters $d_{in}$ and $\theta_{in}$ coupled into the fibre are closer to the acceptance limits of the fibre $D_{core}$ and $\arcsin(NA)$ (given earlier) than with the 600 $\mu$m graded-index fibre. The beam diameter $d_{out}$ behind the fibre clearly exceeds the core diameter $D_{core}$, causing the problems mentioned above with the silicone-coated 600 $\mu$m step index fibre, but on the other hand revealing the good quality of the silicone buffer.

Over a wide range of pumping powers $P_{pump}$ the beam divergence $\theta_{out}$ behind the 600 $\mu$m graded-index fibre is larger than the corresponding limit of the step index fibre $\arcsin(NA)$ (equation (8)), without the beam diameter $d_{out}$ exceeding the core diameter $D_{core}$ (Fig. 14). The authors trace this observation back to the better mode matching of the laser radiation field with the fibre propagation modes in comparison with the step index fibres. This explanation is also supported by the fact that at high pumping powers $P_{pump}$ the fibre-coupling unit of the step index fibres, essentially a long V-groove in an aluminium block, becomes very hot, although the transmission $P_{fibre}/P_{laser}$ is still near the maximum value; whereas with the fibre-coupling unit of the graded-index fibres, a short hole in a small gold-layered aluminium cylinder, remains cold at otherwise comparable conditions.

Finally, considering the requirements on the adjustment precision of the fibre when coupling a high power laser beam into the fibre, the experiments show that step index fibres are very sensitive to small adjustment errors leading to transmission losses or even fibre destruction.

## Fibre end-face preparation

The experiments described in the previous section reveal that the beam divergence $\theta_{in}$ coupled into step index fibres is restricted by the angle $\arcsin(NA)$ (equation (8)), which is different from theory, and which predicts $2\arcsin(NA)$ (equation (4)). Therefore, the influence of the fibre end face preparation on the coupling conditions and transmission properties is investigated.

Two methods of fibre end face preparation are applied. One is to strip off the buffer with a lighter or a sharp scalpel and to remove the residues with an optic paper moistened with an alcohol. Afterwards, the bare fibre is clamped in a metallic plate, with the fibre tip protruding because of its own weight, the clamp construction or light pressure. The plate, including the fibre, is polished several times by hand on polishing paper containing differently-sized fine grains, also moistened with an alcohol. This procedure is applied to all fibres. The 400 $\mu$m step index fibre is usually cleaved—the second method—with a fibre cleaver, adapted to the fibre by the

manufacturer, the York company. The application of the cleaver is limited to this fibre size.

With the first method the fibre gets a slightly spherical end face, thus reducing the theoretical, maximum acceptance angle $2\arcsin(NA)$ (equation (4)). The second method leads to a plane surface. The radius of the end face sphere is estimated by observing the reflection pattern of a HeNe laser aimed at the fibre end face at a small angle.[9] The estimation yields a reduction of the theoretical acceptance angle $2\arcsin(NA)$ of less than 7%, which cannot explain the high transmission losses described earlier (see Figs 9 and 10). When simultaneously coupling a high power laser beam into the fibre, thus observing a possible increase of the radius of the spherical end face, the reflection pattern does not change. Furthermore, there is no significant difference concerning maximum beam power $P_{\text{laser}}$ and transmission $P_{\text{fibre}}/P_{\text{laser}}$ when comparing the 400 $\mu$m step index fibres being prepared according to the two methods.

Finally, the numerical aperture $NA$ itself, of the 400 $\mu$m step index fibre is checked. The light of a halogen lamp is focused onto the fibre end face with a similar telescopic system, as used for high power laser transmission, yielding a beam diameter $d_{\text{in}}$ at the fibre end face of about 1 mm and a divergence $\theta_{\text{in}}$ of approximately 300 mrad, thus completely filling the fibre core with light. With bending of the fibre, with a radius of about 1 cm, several times in two opposite directions around mandrels, stripping the buffer off at 20 cm length behind it and laying the bare fibre in glycerin (having a refractive index higher than that of the silica cladding) the radiation field in the fibre core is homogenized. The diameter $d_{\text{out}}$ of the radiation field, measured behind the fibre, is 402 $\mu$m, the divergence $\theta_{\text{out}}$ 444 mrad, which gives a very good approximation of the values of the fibre core diameter $D_{\text{core}}$ and the acceptance angle $2\arcsin(NA)$. Because no reliable measurements of transmission losses can be carried out, it is not possible to discuss further the validity and limits of the numerical aperture $NA$.

## Conclusions

The maximum laser power of a multimode high power laser beam transmitted through step index fibres is limited by the beam parameters. The beam diameter at the input fibre end face may not exceed the core diameter of the fibre, the beam divergence shall not be larger than half the acceptance angle $\arcsin(NA)$, using the 98% definition for the beam diameters. Beams with higher divergence suffer increasing transmission losses because of the mismatch of the laser radiation field with the fibre propagation modes. The propagation modes of graded-index fibres are better matched with the laser radiation field, thus leading to more laser power transmitted and higher transmission values. The graded-index fibres under investigation have a silicone buffer of good optical quality, which further diminishes the transmission losses. If part of the laser power is not confined in the fibre core, it can be guided in the cladding because of the lower refractive index of the buffer material. There is no significant difference between polished and cleaved step index fibres, although the latter procedure leads to spherical fibre end faces, which reduce the acceptance angle $\arcsin(NA)$ by less than 10%.

## Acknowledgement

The authors thank Professor H. Weber, Technische Universität Berlin, Germany, and Mr. M. Kumkar, Festkörper-Laser-Institut Berlin GmbH, Germany, for numerous discussions, Mr. H. Lemanski, Technische Hochschule Ilmenau, Germany, for doing the fibre end face preparations and performing many of the measurements, Professor K.-H. Klein, Fachhochschule Gießen-Friedberg, Germany, Dr K.-H. Schönborn and Dr H. C. Bader, Schott Glaswerke, Germany, for many hints. This work was supported by BMFT contract EU 226, phase 2.

## References

1 **Ishide, T., Matsumoto, O., Nagura, Y., Nagashima, T.** Optical fiber transmission of 2 kW cw YAG laser and its practical application to welding, *Proc SPIE* **1277,** (1990) 188–198.
2 **Göller, E., Huber, R., Iffländer, R., Schäfer, P., Wallmeroth, K.** Solid state 2 kW-cw-laser: Results of a task being part of the EUREKA-project EU 226, HAAS-LASER, Schramberg, Germany, January 1992.
3 **Burrows, G., Croxford, N., Hoult, A. P., Ireland, C. L. M., Weedon, T. M.** Welding characteristics of a 2 kW YAG laser, *Proc SPIE* **1021,** (1988) 159–166.
4 **Tönshof, H. K., Meyer-Kobbe, C., Beske E.** New possibilities in material processing with kW-solid state lasers, *Proc SPIE* **1277,** (1990) 199–208.
5 **Murata, H.** *Handbook of Optical Fibers and Cables*, Marcel Dekker, New York, (1988).
6 **Driedger, K. P., Iffländer, R. M., Weber, H.** Multirod resonators for high-power solid-state lasers with improved beam quality, *IEEE J Quant Electron* **24,** (1988) 665–673.
7 **Kumkar, M., Wedel, B., Richter, K.** Beam quality and efficiency of high-average-power multirod lasers, *Opt Laser Technol* **24,** (1992) 67–72.
8 **Reng, N., Eppich, B.** Definition and measurements of high power laser beam parameters, *Optical and Quantum Electron* **24,** (1992) 5973–5992.
9 **Beck, T.** Übertragung hoher Lichtleistungen durch Glasfasern, diploma dissertation, Optisches Institut, TU Berlin, (1992).
10 **Hodgson, N.** *Optische Resonatoren für Hochleistungs-Festkörper-Laser*, Internal report, Festkörper-Laser-Institut Berlin GmbH, Germany, (1990).
11 **Marcuse, D.** Coupling coefficients of coupled laser cavities, *IEEE J Quant Electron* **22,** (1986) 223–226.
12 **Lang, R. J., Yariv, A.** An exact formulation of coupled-mode theory for coupled-cavity lasers, *IEEE J Quant Electron* **24,** (1988) 66–72.
13 **Snyder, A. W., Love, J. D.** *Optical Waveguide Theory*, Chapman and Hall, London, (1983).
14 **Okoshi, T.** *Optical Fibers*, Academic Press, Orlando, (1982).
15 **Snyder, A. W., Pask, C., Mitchell, D. J.** Light-acceptance property of an optical fiber, *J Opt Soc Am* **63,** (1973) 59–64.
16 **Marcuse, D.** *Light Transmission Optics*, Van Nostrand Reinhold, New York, (1982).
17 **Kawakami, S., Nishizawa, J.-I.** An optical waveguide with the optimum distribution of the refractive index with reference to waveform distortion, *IEEE Trans Microwave Theory and Techniques* **16,** (1968) 814–818.
18 **Snyder, A. W.** Excitation and scattering of modes on a dielectric or optical fiber, *IEEE Trans Microwave Theory and Techniques* **17,** (1969) 1138–1144.
19 **Gloge, D.** Propagation effects in optical fibers, *IEEE Trans Microwave Theory and Techniques* **23,** (1975) 106–120.
20 **Unger, H.-G.** *Planar Optical Waveguides and Fibres*, Clarendon Press, Oxford, (1977).
21 **Siegman, A. E.** *Lasers*, University Science Books, Mill Valley, California, (1986).